

Absence of Odd-Even Parity Behavior for Kondo Resonances in Quantum Dots

J. Schmid, J. Weis, K. Eberl, and K. v. Klitzing

Max-Planck-Institut für Festkörperforschung, Heisenbergstrasse 1, D-70569 Stuttgart, Germany
(Received 10 November 1999)

Zero-bias anomalies in the conductance through quantum dots have recently been identified as Kondo resonances and explained in terms of the Anderson impurity model. The effect requires a degeneracy and it has been proposed that this should occur for odd electron numbers on the dot. In this paper we present data, obtained on a split-gate quantum dot with a small number of electrons, which are in disagreement with this expectation. The mapping of the Anderson model on the quantum dot is discussed in terms of an interacting N electron system demonstrating why this expectation can fail.

PACS numbers: 73.23.Hk, 72.15.Qm, 73.20.Dx, 75.20.Hr

In 1961, Anderson [1] introduced a simple model to describe the interaction of magnetic impurities with conduction band electrons of a metal, leading to the Kondo effect. In 1988, it was recognized [2,3] that this Anderson impurity model could be applied to a quantum dot (QD) coupled to two electron reservoirs. Theories have been developed to describe this system even in the nonequilibrium situation of an applied bias voltage between the reservoirs [4–6]. Experimentally, signatures of Kondo resonances in quantum dots have recently been found [7–9]. It was claimed that the effect should be present for any odd number of electrons on the dot (see, for instance, [10,11]). This expectation was confirmed by some experimental results [7,8]. In this Letter, we report on experimental results showing the absence of odd-even behavior in our quantum dots.

Our sample is based on a GaAs/Al_{0.33}Ga_{0.67}As heterostructure with a two-dimensional electron system (2DES) at the GaAs-AlGaAs heterojunction 50 nm below the surface [12]. A Hall bar is defined by wet etching and the 2DES is contacted by alloying AuGeNi pads. Metal gates consisting of a 5 nm thick NiCr and a 20 nm Au layer are deposited across the Hall bar using e-beam evaporation and a lift-off process on a pattern defined by electron beam lithography. Figure 1(a) shows a scanning electron microscope (SEM) image of the central gate region. The open area between the gate fingers is about 180 nm in diameter. By applying appropriate negative voltages to these gates, a nearly isolated region (QD) forms in the 2DES between the gate fingers. In the experiments presented here, the outer pairs of gate fingers are kept at fixed voltages of -0.65 and -0.54 V, respectively, allowing tunnel coupling between the dot and the 2DES regions on “left” and “right” [see Fig. 1(a)]. These 2DES regions act as the source and drain leads to the dot, where the drain-source voltage V_{DS} is applied via the alloyed Ohmic AuGeNi contacts. The voltage V_G applied to the middle gate fingers is used to vary the electrostatic potential and, therefore, the number of electrons on the dot. The differential conductance through the QD is measured in a four-terminal arrangement using lock-in amplifiers, an ac excitation of $0.95 \mu\text{V}$ rms amplitude, and a frequency of 37 Hz which is superimposed to the dc bias V_{DS} . The measurements presented here are

done in a ^3He - ^4He dilution refrigerator—when not stated differently—at the base temperature of 15 mK [13].

Without tunnel coupling to the leads, N electrons confined in the QD have a total energy spectrum $E(N, k; \{V_i\})$ which can be labeled by the parameter k , where $k = 0$ denotes the ground state of the N electron system. The total energy spectrum depends, aside from other parameters, on the voltages V_i applied to the source, the drain, and the gate electrodes surrounding the QD [14]. To describe electron transport through the QD in the regime of weak tunnel coupling to the leads, the energies required for adding the $(N + 1)$ th electron into the N electron system (“electron-like” process) and for taking off the N th electron from the QD (“holelike” process) have to be considered. Figure 1(b) shows an energy scheme where the ground state energy differences $\mu(N + 1; \{V_i\}) \equiv E(N + 1, 0; \{V_i\}) - E(N, 0; \{V_i\})$ between the $N + 1$ and the N electron

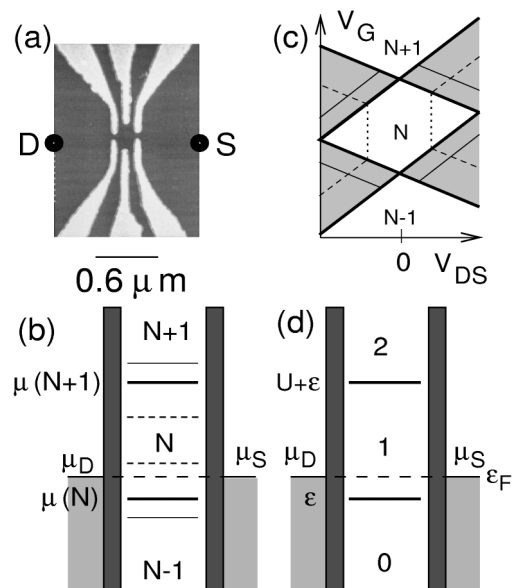


FIG. 1. (a) SEM image of the split-gate electrodes used to define the quantum dot. (b) Energy scheme to describe transport through a QD. (c) Sketch of the regions of SET (dark) and CB (light) in the V_G vs V_{DS} plane. (d) Energy scheme of the Anderson impurity model.

system are plotted for different N , but fixed $\{V_i\}$ relative to the Fermi levels, i.e., the electrochemical potentials μ_S^{elch} and μ_D^{elch} of the source and the drain leads. By changing one of the gate voltages, these energies $\mu(N+1; \{V_i\})$ are—in first approximation—linearly shifted relative to the Fermi levels while the distances $\mu(N+1; \{V_i\}) - \mu(N; \{V_i\})$ remain constant [15]. In the case of $\mu(N+1; \{V_i\}) > \{\mu_S^{\text{elch}}, \mu_D^{\text{elch}}\} > \mu(N; \{V_i\})$, energy barriers for adding and for taking off an electron exist. Therefore, at low temperature the electron transport is blocked and we are in the regime of Coulomb blockade (CB) where the number of electrons on the QD is fixed to N [15]. Whenever $\mu(N+1; \{V_i\})$ lies between the Fermi levels of source and drain leads, the number of electrons on the QD is fluctuating between N and $N+1$, and single-electron tunneling (SET) through the QD between source and drain contact can occur [15]. In Fig. 1(c), the CB and SET regimes are sketched as a function of the source-drain voltage V_{DS} and a gate voltage V_G . The boundaries between the regimes are determined by the condition that the energies $\mu(N+1; \{V_i\})$, $\mu(N; \{V_i\})$, etc. are either aligned with μ_S^{elch} or μ_D^{elch} . Within the SET regimes at finite drain-source voltage $eV_{\text{DS}} = \mu_D^{\text{elch}} - \mu_S^{\text{elch}}$, additional channels in the transport through the QD become available, which have been related to excited states of the confined N and $N+1$ electron systems. Such transport spectroscopy of excited energy states given by $E(N+1, k; \{V_i\}) - E(N, l; \{V_i\})$ has been described [15] and used in the past. Applied to our QD, this shows that a well-developed discrete energy spectrum exists in our QD.

Figure 2(a) presents experimental data of the differential conductance through our QD as a function of V_{DS} and V_G around two adjacent regions of Coulomb blockade, but already for the case of stronger tunnel coupling to the leads. The boundary lines between CB and SET are smeared out due to the finite lifetime of the electrons on the dot, but still clearly visible. Remarkable is the appearance of a strong differential conductance peak $dI_{\text{DS}}/dV_{\text{DS}} > e^2/h$ around $V_{\text{DS}} = 0$ where—in the weak tunnel coupling regime—single-electron transport is blocked (CB regime). With increasing temperature, this peak disappears as shown in Figs. 2(b) and 2(c) [16]. Such a zero-bias anomaly has been predicted and calculated [4–6] by using the so-called Anderson impurity model [1]: The Hamiltonian of the extended Anderson impurity model [sketched in Fig. 1(d)] describes one spin degenerate energy level coupled by tunneling to two electron reservoirs containing electrons of both spin orientations. On the impurity site, an electron has the energy ε which lies below the Fermi level ε_F . Occupation of the impurity site by two electrons at the same time is suppressed due to the electron-electron interaction energy U on this site. The prediction for this simple model is that correlated virtual tunneling processes between dot and reservoir(s) lead to a sharp peak in the effective density of states (spectral function) [4,6] at the impurity site pinned to the Fermi energy of the reservoir(s), if the temperature of the system is below the so-called Kondo

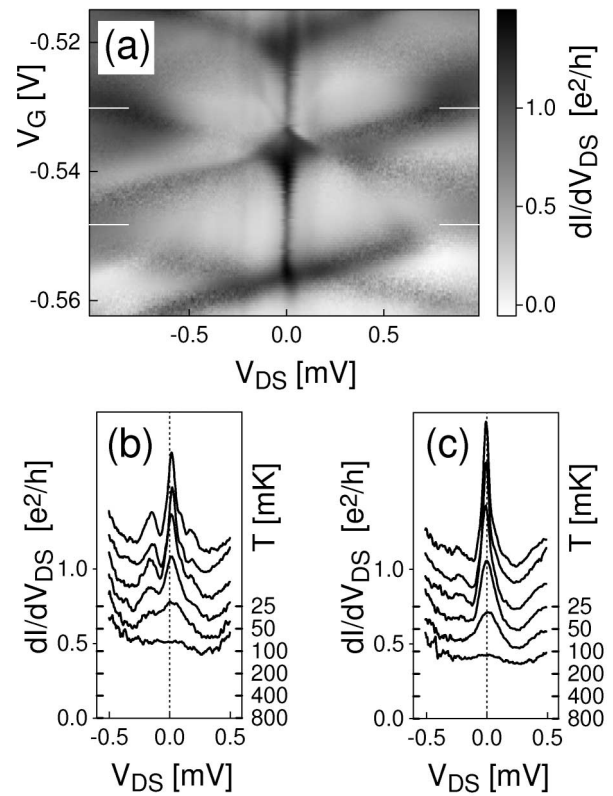


FIG. 2. (a) Differential conductance dI/dV_{DS} as a function of V_G and V_{DS} ; Kondo resonances are observed in two consecutive CB regions. (b) Curves taken at different temperatures and fixed V_G in the *middle* of the upper CB valley and (c) of the lower CB valley [the V_G values are marked by white lines in (a)]. The curves in (b) and (c) are offset, the ticks next to the temperature value mark zero dI/dV_{DS} .

temperature. This critical temperature depends on the tunnel coupling strength and the position of ε below ε_F . This effective density of states, at the Fermi level on the impurity site, leads to a peak in the differential conductance through the impurity at $V_{\text{DS}} = 0$, denoted as a Kondo resonance, even though $\varepsilon < \varepsilon_F$ and $\varepsilon + U > \varepsilon_F$.

The mapping of the Anderson model to the QD will work under the following conditions: (i) The energies ε and $\varepsilon + U$ of the Anderson model are identified with the energies $\mu(N; \{V_i\})$ and $\mu(N+1; \{V_i\})$, respectively. The degeneracy within the Anderson model corresponds to a degeneracy of the N electron system; i.e., there are two states $|N, 0\rangle$ and $|N, 1\rangle$ at the ground state energy with $E(N, 1; \{V_i\}) - E(N, 0; \{V_i\}) = 0$, for instance, due to spin degeneracy. Since this is expected to occur only for certain N , the mapping will work only for certain CB regions. (ii) Although in our QD the electron number N is not equal to one, the fluctuations in the electron number are restricted. In the energetical situation depicted in Fig. 1(b), N is the most likely value, $N \pm 2$ (which do not occur in the Anderson impurity model) are strongly suppressed if the energies $|\mu(N+2; \{V_i\}) - \mu(N+1; \{V_i\})|$ and $|\mu(N; \{V_i\}) - \mu(N-1; \{V_i\})|$ are large compared to the thermal energy $k_B T$ and the level

broadening Γ due to the tunnel coupling. These conditions are well fulfilled in our experiment. (iii) Corrections due to excited states of the N electron system can be neglected under the condition that their energetical separation from the ground state is large compared to $k_B T$ and Γ . This last condition is *not* fulfilled in our QD; there exist low lying excitations [18]. In such a case, the Kondo resonance can also be expected if the N electron system is *not* degenerate at its ground state energy, but at a low lying excitation energy.

In the experiment, the degeneracy can be lifted by applying a magnetic field, i.e., $E(N, 1; \{V_i\}) - E(N, 0; \{V_i\}) = \Delta\varepsilon$, and split Kondo resonances are observed [7–9]. In Fig. 1(c), which schematically shows the SET and CB regions in the V_G vs V_{DS} plane, the split Kondo resonances are expected along the vertical lines through the CB region at $V_{DS} = \pm\Delta\varepsilon/e$ [4,21]. Both zero-bias anomalies shown in Fig. 2(a) split with the parallel magnetic field as expected for lifting a spin degeneracy by Zeeman splitting—in agreement with recent measurements [22] where the magnetic field orientation is tilted from parallel to perpendicular to the plane of the 2DES.

In several papers [7,8], an odd-even parity behavior with the number of electrons in the QD has been reported for the occurrence of Kondo resonances. Obviously, this is not the case for our QD where we observe the zero-bias anomaly in two adjacent CB regimes [see Fig. 2(a)], i.e., for N_0 and $N_0 + 1$. This experimental result demonstrates that the expectation of an odd-even behavior in the occurrence of Kondo resonances is based on assumptions which are not fulfilled in our experiments—in none of five quantum dots studied, all of which showed at least one Kondo resonance. One critical assumption is the so-called constant interaction (CI) model [19,23] where the electron-electron interaction on the dot is taken to be constant—described by a capacitance—and where a single-particle energy spectrum is assumed which does not depend on the electron number. When filling up single-particle levels which are spin degenerate, the highest electron level is half-filled for odd electron numbers. In this case, the Anderson impurity model is applicable in its original form and a Kondo resonance is expected. A possible orbital degeneracy is explicitly ignored based on the argument that quantum dots lack symmetry.

The invalidity of the CI model is clearly visible in a number of experiments on small QDs: (i) Transport experiments on QDs defined in III-V semiconductor heterostructure pillars have shown that Hund's rule is necessary to explain the experimental results [20,24]. Instead of filling up the levels with spin-up and spin-down electrons consecutively, parallel spin configurations are favorable due to exchange interaction. The odd-even behavior in N for the occurrence of Kondo resonances should be broken in such a case. (ii) In QDs of few electrons where the electron-electron interaction is dominating over the confinement energy, correlation effects due to electron-electron interaction have to be taken into account [25,26]: The degeneracy of

the ground state energy of the N -electron system is not expected to change in an obvious odd-even manner with N .

To learn more about the energy spectrum of our QD, magnetic field dependent measurements have been performed. In Fig. 3, the conductance around $V_{DS} = 0$ —measured by the lock-in technique—is presented as a function of the gate voltage V_G and of the magnetic field B , applied perpendicular to the plane of the 2DES. Along the gate voltage axis, the electron number in the QD is changed by one whenever crossing a SET conductance peak. This happens at V_G , for which $\mu_D^{\text{elch}} \approx \mu(X; V_G, B) \approx \mu_S^{\text{elch}}$ with $X = \dots, N-1, N, N+1, \dots$. At $V_G > -0.5$ V and low magnetic fields, such SET conductance peaks are not resolvable due to the strong tunnel coupling to the leads. They are, however, observable in this gate voltage regime at higher magnetic fields where the tunnel coupling has diminished with increasing the magnetic field. Following the SET peak of, for instance, $\mu_D^{\text{elch}} \approx \mu(N+1; V_G, B) \approx \mu_S^{\text{elch}}$ along the magnetic field axis, wiggles in the gate voltage position of the SET peak are visible, which indicate a change in the ground state of either the N or the $N+1$ electron system on the QD [15]. Visible is also a variation of the conductance in the valley *between* the SET conductance peaks—the regimes which are denoted in the weak tunnel coupling regime as CB regions. The variations in the valleys are clearly related to the wiggles observed for the SET peaks; i.e., they are related to changes in the electronic states of the QD. The Coulomb blockade regimes, where the Kondo resonances presented in Fig. 2 are observed, are marked by N_0 and $N_0 + 1$ in Fig. 3. Counting the spin flips observed at higher fields results in the estimate $N_0 = 7$ and $N_0 + 1 = 8$.

In Fig. 3, it is immediately evident that there is an odd-even effect in the valley conductance along the dotted line. This is also observable in other regions in this plot.

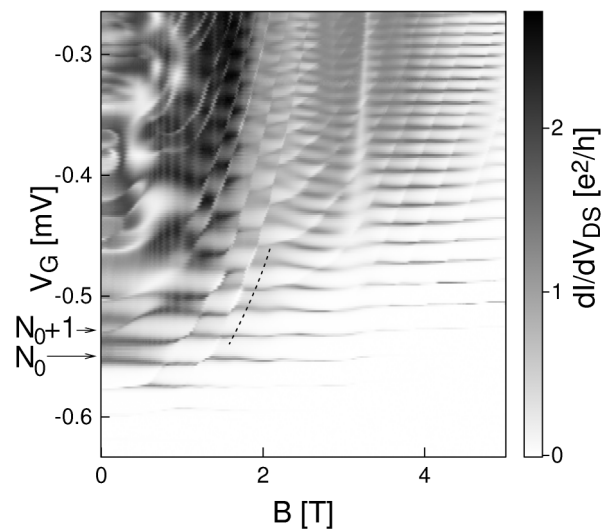


FIG. 3. Differential conductance dI/dV_{DS} as a function of the magnetic field B perpendicular to the 2DES and the gate voltage V_G .

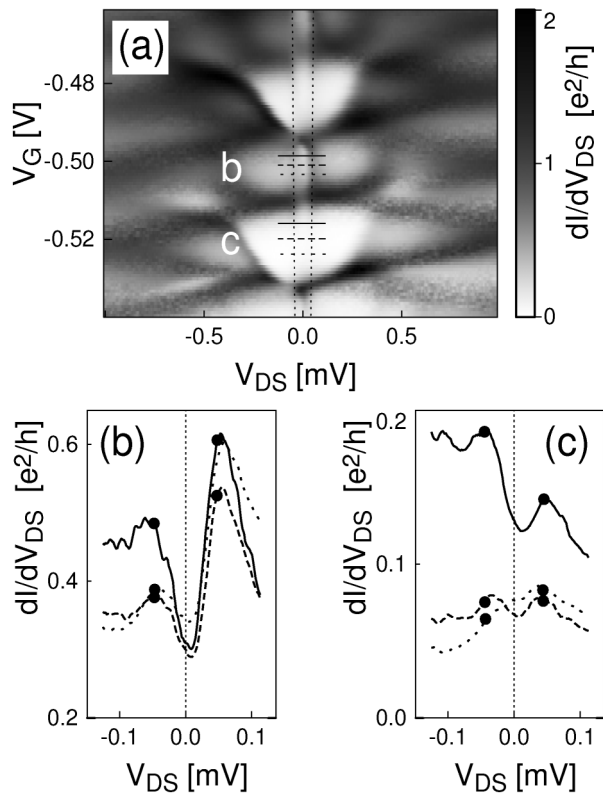


FIG. 4. (a) Differential conductance in gray scale as a function of V_{DS} and V_G (b) following the line given in Fig. 3. Maxima in the high conductance valleys at the position of the spin splitting (dashed lines) are visible. (b), (c) Traces of the differential conductance in a high (b) and a low (c) conductance valley. The gate voltages are marked by the horizontal lines in (a). The dots mark the value of the spin splitting for the respective curves.

Furthermore, this is not an effect in the total electron number N : By shifting the line in Fig. 3 to the left, high and low conductance valleys are interchanged. Since a finite magnetic field is applied, a suspected spin degeneracy is lifted due to Zeeman splitting. Therefore, two Kondo peaks at *finite* $V_{DS} = \pm g_{\text{GaAs}} \mu_B B / e$ are expected, symmetric with respect to $V_{DS} = 0$. To check this expectation, differential conductance measurements have been performed along the dotted line shown in Fig. 3. The results are presented in Fig. 4 as a function of V_{DS} and V_G . Indeed, the splitting fits to the Zeeman energy at these B values and is observed for the valley of high conductance, but also for the valley of low conductance: Split Kondo resonances are seen in each of these valleys, although N is increased one by one.

Let us suppose that there is an odd-even effect in Fig. 4 with the increasing of the electron number in the occurrence of the spin degeneracy at the ground state energy. This would explain the well-developed split resonances in the high conductance valleys, but not the observation in

the low conductance valleys. Whether a degeneracy of an excited state is responsible for this has still to be clarified.

In conclusion, we have experimentally observed deviations from an odd-even behavior in the electron number for the occurrence of Kondo resonances in a split-gate QD at zero magnetic field. The magnetic field dependent measurement shows a nice energy spectrum indicating a low number of electrons in the QD. By discussing the mapping of the Anderson impurity model and a QD with an interacting N electron system, the expectation of an odd-even effect expressed in recent papers is corrected.

This work has been supported by the Bundesministerium für Bildung und Forschung (BMBF) under Grant No. 01 BM 624/7.

- [1] P. W. Anderson, *Phys. Rev.* **124**, 41 (1961).
- [2] L. I. Glazman and M. É. Raïkh, *JETP Lett.* **47**, 452 (1988).
- [3] T. K. Ng and P. A. Lee, *Phys. Rev. Lett.* **61**, 1768 (1988).
- [4] Y. Meir *et al.*, *Phys. Rev. Lett.* **70**, 2601 (1993).
- [5] A. L. Yeyati *et al.*, *Phys. Rev. Lett.* **71**, 2991 (1993).
- [6] J. König *et al.*, *Phys. Rev. Lett.* **76**, 1715 (1996).
- [7] D. Goldhaber-Gordon *et al.*, *Nature (London)* **391**, 156 (1998).
- [8] S. M. Cronenwett *et al.*, *Science* **281**, 540 (1998).
- [9] J. Schmid *et al.*, *Physica (Amsterdam)* **256B–258B**, 182 (1998).
- [10] A. Kawabata, *J. Phys. Soc. Jpn.* **60**, 3222 (1991).
- [11] Yi Wan *et al.*, *Phys. Rev. B* **51**, 14 782 (1995).
- [12] Layer sequence from surface to substrate: 10 nm GaAs cap, 20 nm $\text{Al}_{0.33}\text{Ga}_{0.67}\text{As}$:Si continuously doped, 20 nm $\text{Al}_{0.33}\text{Ga}_{0.67}\text{As}$ spacer, 500 nm GaAs, and buffer layers.
- [13] The actual electron temperature is found to be higher: for appropriate parameters the Kondo peaks show logarithmic temperature dependence down to 50 mK and no temperature dependence below 25 mK.
- [14] L. D. Hallam *et al.*, *Phys. Rev. B* **53**, 1452 (1996).
- [15] J. Weis *et al.*, *Semicond. Sci. Technol.* **9**, 1890 (1994).
- [16] In Fig. 2(b), side peaks are visible that may require excited states [17] as an explanation.
- [17] Takeshi Inoshita *et al.*, *Superlattices Microstruct.* **22**, 75 (1997).
- [18] The energy separation between the ground state and the excited state of the interacting N electron system can be lower than the single-particle level spacing (see, for instance, the total energy spectrum of one, two, and three electrons interacting in a parabolic confinement potential [25,26]).
- [19] D. A. Averin *et al.*, *Phys. Rev. B* **44**, 6199 (1991).
- [20] S. Tarucha *et al.*, *Phys. Rev. Lett.* **77**, 3613 (1996).
- [21] J. König *et al.*, *Phys. Rev. B* **54**, 16 820 (1996).
- [22] J. Schmid *et al.*, *Physica E* (to be published).
- [23] C. W. J. Beenakker, *Phys. Rev. B* **44**, 1646 (1991).
- [24] T. H. Oosterkamp *et al.*, *Phys. Rev. Lett.* **82**, 2931 (1999).
- [25] U. Merkt *et al.*, *Phys. Rev. B* **43**, 7320 (1991).
- [26] D. Pfannkuche *et al.*, *Phys. Rev. Lett.* **74**, 1194 (1995).